Spin-Lattice Relaxation at Zero Magnetic Field. I. Phenomenological Theory of Relaxation among Hyperfine Levels*

E. R. Bernstein and D. R. Franceschetti†
Department of Chemistry, Princeton University, Princeton, New Jersey 08540
(Received 10 February 1972)

Spin-lattice relaxation at zero external magnetic field is studied for the Kramers ions Nd^{3+} and Er^{3+} in both lanthanum trichloride, $LaCl_3$, and lanthanum ethyl sulphate, $La(C_2H_5SO_4)_3 \cdot 9H_2O$, in the 1–15-K temperature range. Employing a phenomenological theory which treats the crystal lattice-ion interaction as the first term in a Taylor-series expansion of the crystal field potential, we find a negligible direct- (one-phonon) process transition probability proportional to T, a Raman-process transition probability proportional to T^7, and a resonance Raman-(Orbach-) process transition probability proportional to $e^{-\Delta/kT}$. The multilevel zero-field problem is solved using matrix techniques. It is found that some levels return to equilibrium in an almost-single-exponential fashion, while others can be discussed in terms of a sum of up to seven exponentials. Both long- and short-pulse experiments are discussed.

I. INTRODUCTION

Zero-field paramagnetic resonance is a promising technique for high-resolution study of low-lying and optically excited energy levels of many paramagnetic ions and molecules in crystals.[1,2] In connection with experimental studies underway on spin-lattice relaxation at zero field, we consider here relaxation of a system of hyperfine levels at zero external magnetic field. Spin-lattice relaxation of ions with hyperfine structure has been of special interest in connection with electron-nuclear-double-resonance (ENDOR) experiments, dynamic nuclear orientations,[3,4] and electron-paramagnetic–electron-paramagnetic-double-resonance experiments.[5] An immense amount of work has been published on spin-lattice relaxation in electron paramagnetic resonance and nuclear magnetic resonance.[3,4,6] While qualitative details appear to be understood, numerical agreement with experiment leaves much to be desired in many instances. It is our hope that studies of relaxation at zero magnetic field will contribute to the development of this theory in general, as well as elucidate particular features of the unique zero-field situation.

The phenomenological theory due mainly to Orbach[7] provides the basis for most work done on paramagnetic relaxation of rare-earth ions in solids. As a first step in understanding zero-field relaxation, we have adapted this theory to the hyperfine levels of four systems: $LaCl_3:Nd^{3+}$, $LaES:Nd^{3+}$, $LaCl_3:Er^{3+}$, and $LaES:Er^{3+}$, where LaES stands for $La(C_2H_5SO_4)_3 \cdot 9H_2O$. We believe a phenomenological theory will account for the qualitative features of zero-field-relaxation measurements in these systems. In the near future we will present a more rigorous theory of spin-lattice relaxation at zero field based on more formal solutions of the Liouville equation for the ion-lattice density matrix. Zero-field paramagnetic relaxation for a Kramers electronic ion with hyperfine structure evidences some interesting features which we feel are worth noting even though presented in an approximate or phenomenological framework. We have chosen this vehicle initially in order to underscore the general nature of the zero-field-relaxation problem both with regard to the processes involved and the difficulty of dealing with multilevel, coupled, relaxing manifolds of states. These problems will, of course, also be central to any more sophisticated mechanistic approach.

In order to make a clean separation between the various parts of this work so that subsequent theory can readily build on appropriate material in this paper, we have divided the presentation into several distinct parts. In Sec. II of this paper we derive the electronic and hyperfine levels involved. This is followed in Sec. III by a discussion of mathematical techniques used in handling relaxation in a many-level system with degenerate levels. Section IV contains a discussion of spin-lattice interaction. In Sec. V transition probabilities for direct, Raman, and resonance Raman (Orbach) processes are discussed and presented. We conclude with a statement of predicted experimental results.

II. ELECTRONIC AND HYPERFINE LEVELS

The ground state of Nd^{3+} is $4f^3$, $^4I_{9/2}$ with the nearest excited state $^4I_{11/2}$ removed by 1800 cm^{-1}, while Er^{3+} has a ground state $4f^{11}$, $^4I_{15/2}$ and first excited state $^4I_{13/2}$ removed by 8000 cm^{-1}. Therefore J, the total electronic angular momentum, is approximately a good quantum number even in a nonspherical crystal environment. Within this approximation [actually $\xi(r)\vec{L}\cdot\vec{S} \gg V_{cf}$] the Hamiltonian for the ion in a crystal field may be written

$$\mathcal{H}=\sum_{n,m} A_n^m \langle r^n\rangle \chi_n O_n^m(J)+\sum_m A_{\rm nuc}^m O_2^m(I) + \mathcal{H}_{\rm hf}+\mathcal{H}_{\rm quad} . \quad (2.1)$$

The O_n^m and χ_n are the usual operator equivalents and proportionality factors (most of the operator equivalents for $n=2, 4, 6$ have been tabulated by Abragam and Bleaney,[3] the remainder are presented by Buckmaster[8]). The first term in (2.1) is the usual crystal field term; the second term represents the crystal field interaction with the nuclear quadrupole moment (the effect of core polarization is included in the constants $A_{\rm nuc}^m$); $\mathcal{H}_{\rm hf}$ is the usual magnetic hyperfine term; and $\mathcal{H}_{\rm quad}$ represents the interaction of the nuclear quadrupole moment with the unpaired-electron distribution.

In what follows we will make some use of the transformation properties of the Hamiltonian. The first two terms in (2.1) have the same transformation properties as the crystal field potential; that is, they transform totally symmetrically under the site-group operations. The last two terms transform as the representation $\mathfrak{D}_0$ of the rotation group. We write such terms using irreducible spherical tensor operators Q_n^m. O_n^m and Q_n^m are then related by

$$g_n^{|m|} O_n^m=(-1)^m Q_n^m+Q_n^{-m} , \quad (2.2)$$

in which the $g_n^{|m|}$ have been tabulated by Scott and Jeffries.[9] Requiring $\mathcal{H}_{\rm hf}$ and $\mathcal{H}_{\rm quad}$ to transform as scalars[10] ($\mathfrak{D}_0$ of the rotation group), we have

$$\mathcal{H}_{\rm hf}=\alpha' \sum_m \langle 11\,00|\,1m\,1-m\rangle\, Q_1^m(J)\, Q_1^{-m}(I) \quad (2.3)$$

and

$$\mathcal{H}_{\rm quad}=P'_{\rm quad} \sum_m \langle 22\,00|\,2m\,2-m\rangle\, Q_2^m(J)\, Q_2^{-m}(I) . \quad (2.4)$$

The Clebsch-Gordan coefficients in (2.3) and (2.4) are easily evaluated:

$$\langle 11\,00|\,1m\,1-m\rangle=(-1)^m/\sqrt{3} ,$$

$$\langle 22\,00|\,2m\,2-m\rangle=(-1)^m/\sqrt{5} ,$$

leading to the conventional forms

$$\mathcal{H}_{\rm hf}=\alpha(\vec{\mathbf{I}}\cdot\vec{\mathbf{J}}) , \quad (2.5)$$

$$\mathcal{H}_{\rm quad}=P_{\rm quad}\{[3J_z^2-J(J+1)][3I_z^2-I(I+1)] + \tfrac{3}{2}[(J_zJ_++J_+J_z)(I_zI_-+I_-I_z)+(J_zJ_-+J_-J_z) \times (I_zI_++I_+I_z)]+\tfrac{3}{2}(J_+^2I_-^2+J_-^2I_+^2)\} . \quad (2.6)$$

In axial symmetry the crystal field term reduces to the form (employing conventional operator equivalents and not irreducible spherical tensors)

$$\mathcal{H}_{\rm cf}=A_2^0\alpha\langle r^2\rangle O_2^0+A_4^0\beta\langle r^4\rangle O_4^0+A_6^0\gamma\langle r^6\rangle O_6^0 + A_6^6\gamma\langle r^6\rangle O_6^6 . \quad (2.7)$$

The values of these parameters for the four salts studied are given in Table I and the resulting electronic wave functions are listed in Table II. In crystals of axial, but no higher, symmetry, diagonalizing the crystal field Hamiltonian results in electronic levels which are only doubly degenerate, as required by Kramers theorem.[3] The eigenfunctions are of the form (anticipating the introduction of the effective spin formalism)

$$|\pm\tfrac{1}{2}^n\rangle=C_1|\pm M_J^n\rangle+C_2|\pm M_J^n\pm 6\rangle+C_3|\pm M_J^n\mp 12\rangle . \quad (2.8)$$

The superscript n is used to designate different Kramers doublets. Of course, the axially symmetric crystal field potential requires energy levels (for an odd-electron system) to be doubly degenerate.

Hyperfine states for the electronic ground state, neglecting admixtures of excited electronic states through terms (2.5) and (2.6), can be described by an effective zero-field spin Hamiltonian

$$\mathcal{H}=AS_zI_z+\tfrac{1}{2}B(S_+I_-+S_-I_+)+P[I_z^2-\tfrac{1}{3}I(I+1)] . \quad (2.9)$$

The spin Hamiltonian parameters are given by

$$A=\alpha\langle\tfrac{1}{2}|J_z|\tfrac{1}{2}\rangle/\langle\tfrac{1}{2}|S_z|\tfrac{1}{2}\rangle , \quad (2.10a)$$

$$B=\alpha\langle\tfrac{1}{2}|J_+|-\tfrac{1}{2}\rangle/\langle\tfrac{1}{2}|S_+|-\tfrac{1}{2}\rangle , \quad (2.10b)$$

$$P=3A_{\rm nuc}^0+3P_{\rm quad}\langle\tfrac{1}{2}|Q_2^0(J)|\tfrac{1}{2}\rangle . \quad (2.10c)$$

Since (2.9) approximates an "effective electron nucleus spin-spin coupling," it is convenient to use as labels for the hyperfine states eigenvalues of an effective total angular momentum such that

$$\vec{\mathbf{F}}=\vec{\mathbf{S}}+\vec{\mathbf{I}} , \qquad F_z=S_z+I_z .$$

The spin Hamiltonian then factors into block diagonal form, each block being either 2×2 or 1×1 and corresponding to an eigenvalue of F_z. Hyperfine eigenstates are of the form

TABLE I. Crystal field parameters used in the calculation of electronic wave functions and in estimating the dynamic crystal field parameters. See Eqs. (2.7) and (4.5).

System	$A_2^0\langle r^2\rangle$ (cm^{-1})	$A_4^0\langle r^4\rangle$ (cm^{-1})	$A_6^0\langle r^6\rangle$ (cm^{-1})	$A_6^6\langle r^6\rangle$ (cm^{-1})
$LaCl_3$: Nd[a,b]	97.59	−38.67	−44.44	443.00
LaES: Nd[c]	58.4	−68.2	−42.7	595.0
$LaCl_3$: Er[d,b]	93.89	−37.28	−26.56	265.23
LaES: Er[e]	118.8	−73.9	−30.4	375.9

[a] J. C. Eisenstein, J. Chem. Phys. 39, 2134 (1963).
[b] Mixed crystal data.
[c] J. B. Gruber and R. A. Satten, J. Chem. Phys. 39, 1455 (1963).
[d] J. C. Eisenstein, J. Chem. Phys. 39, 2128 (1963).
[e] J. C. Hill and R. G. Wheeler, Phys. Rev. 152, 482 (1966).

$$|F M_F\rangle = a(M_F)\left|\tfrac{1}{2} M_F - \tfrac{1}{2}\right\rangle + b(M_F)\left|-\tfrac{1}{2} M_F + \tfrac{1}{2}\right\rangle \ , \tag{2.11a}$$

degenerate with

$$|F - M_F\rangle = a(M_F)\left|-\tfrac{1}{2} - M_F + \tfrac{1}{2}\right\rangle + b(M_F)\left|\tfrac{1}{2} - M_F - \tfrac{1}{2}\right\rangle \ ; \tag{2.11b}$$

TABLE II. Experimental crystal field splittings and calculated wave functions for (a) $Nd^{3+}(4f^3,\ {}^4I_{9/2})$ in $LaCl_3$ (Ref. 15), (b) Nd^{3+} $(4f^3,\ {}^4I_{9/2})$ in LaES [J. B. Gruber and R. A. Satten, J. Chem. Phys. 39, 1455 (1963)], (c) Er^{3+} $(4f^{11},\ {}^4I_{15/2})$ in $LaCl_3$ [R. C. Mikkelson and H. J. Stapleton, Phys. Rev. 140, A1968 (1965); corrected by G. E. Stedman and D. J. Newman, J. Chem. Phys. 55, 152 (1971)], and (d) Er^{3+} $(4f^{11},\ {}^4I_{15/2})$ in LaES [J. C. Hill and R. G. Wheeler, Phys. Rev. 152, 482 (1966)].

n	$E_n(\mathrm{cm}^{-1})$	Wave functions
		(a)
4	249.4	$0.936\left\|\pm\tfrac{5}{2}\right\rangle - 0.351\left\|\mp\tfrac{7}{2}\right\rangle$
3	244.4	$0.558\left\|\pm\tfrac{9}{2}\right\rangle - 0.830\left\|\mp\tfrac{3}{2}\right\rangle$
2	123.2	$0.830\left\|\pm\tfrac{9}{2}\right\rangle + 0.558\left\|\mp\tfrac{3}{2}\right\rangle$
1	115.4	$\left\|\pm\tfrac{1}{2}\right\rangle$
0	0.0	$0.351\left\|\pm\tfrac{5}{2}\right\rangle + 0.936\left\|\mp\tfrac{7}{2}\right\rangle$
		(b)
4	311	$0.659\left\|\pm\tfrac{9}{2}\right\rangle - 0.752\left\|\mp\tfrac{3}{2}\right\rangle$
3	279	$0.428\left\|\pm\tfrac{7}{2}\right\rangle - 0.904\left\|\mp\tfrac{5}{2}\right\rangle$
2	154	$\left\|\pm\tfrac{1}{2}\right\rangle$
1	149	$0.752\left\|\pm\tfrac{9}{2}\right\rangle + 0.659\left\|\mp\tfrac{3}{2}\right\rangle$
0	0	$0.904\left\|\pm\tfrac{7}{2}\right\rangle + 0.428\left\|\mp\tfrac{5}{2}\right\rangle$
		(c)
7	229.31	$0.876\left\|\pm\tfrac{13}{2}\right\rangle + 0.401\left\|\pm\tfrac{1}{2}\right\rangle + 0.268\left\|\mp\tfrac{11}{2}\right\rangle$
6	181.04	$0.789\left\|\pm\tfrac{11}{2}\right\rangle + 0.431\left\|\mp\tfrac{1}{2}\right\rangle - 0.439\left\|\mp\tfrac{13}{2}\right\rangle$
5	141.61	$0.103\left\|\pm\tfrac{15}{2}\right\rangle + 0.778\left\|\pm\tfrac{3}{2}\right\rangle + 0.620\left\|\mp\tfrac{9}{2}\right\rangle$
4	113.70	$0.657\left\|\pm\tfrac{7}{2}\right\rangle + 0.754\left\|\mp\tfrac{5}{2}\right\rangle$
3	96.52	$0.201\left\|\pm\tfrac{13}{2}\right\rangle - 0.808\left\|\pm\tfrac{1}{2}\right\rangle + 0.552\left\|\mp\tfrac{11}{2}\right\rangle$
2	64.72	$0.829\left\|\pm\tfrac{15}{2}\right\rangle + 0.277\left\|\pm\tfrac{3}{2}\right\rangle - 0.486\left\|\mp\tfrac{9}{2}\right\rangle$
1	37.91	$0.550\left\|\pm\tfrac{15}{2}\right\rangle - 0.564\left\|\pm\tfrac{3}{2}\right\rangle + 0.616\left\|\mp\tfrac{9}{2}\right\rangle$
0	0.0	$0.754\left\|\pm\tfrac{7}{2}\right\rangle - 0.657\left\|\mp\tfrac{5}{2}\right\rangle$
		(d)
7	304.0	$0.86\left\|\pm\tfrac{13}{2}\right\rangle + 0.38\left\|\pm\tfrac{1}{2}\right\rangle + 0.34\left\|\mp\tfrac{11}{2}\right\rangle$
6	255.2	$0.47\left\|\pm\tfrac{13}{2}\right\rangle - 0.32\left\|\pm\tfrac{1}{2}\right\rangle - 0.82\left\|\mp\tfrac{11}{2}\right\rangle$
5	215.8	$0.10\left\|\pm\tfrac{15}{2}\right\rangle + 0.69\left\|\pm\tfrac{3}{2}\right\rangle + 0.71\left\|\mp\tfrac{9}{2}\right\rangle$
4	172.5	$0.69\left\|\pm\tfrac{7}{2}\right\rangle + 0.72\left\|\mp\tfrac{5}{2}\right\rangle$
3	110.1	$0.21\left\|\pm\tfrac{13}{2}\right\rangle - 0.87\left\|\pm\tfrac{1}{2}\right\rangle + 0.45\left\|\mp\tfrac{11}{2}\right\rangle$
2	64.7	$0.86\left\|\pm\tfrac{15}{2}\right\rangle + 0.30\left\|\pm\tfrac{3}{2}\right\rangle - 0.41\left\|\mp\tfrac{9}{2}\right\rangle$
1	44.0	$0.50\left\|\pm\tfrac{15}{2}\right\rangle - 0.65\left\|\pm\tfrac{3}{2}\right\rangle + 0.57\left\|\mp\tfrac{9}{2}\right\rangle$
0	0.0	$0.72\left\|\pm\tfrac{7}{2}\right\rangle - 0.69\left\|\mp\tfrac{5}{2}\right\rangle$

and

$$|F - 1\ M_F\rangle = b(M_F)\left|\tfrac{1}{2} M_F - \tfrac{1}{2}\right\rangle - a(M_F)\left|-\tfrac{1}{2} M_F + \tfrac{1}{2}\right\rangle \ , \tag{2.11c}$$

degenerate with

$$|F - 1 - M_F\rangle = b(M_F)\left|-\tfrac{1}{2} - M_F + \tfrac{1}{2}\right\rangle - a(M_F)\left|\tfrac{1}{2} - M_F + \tfrac{1}{2}\right\rangle \ . \tag{2.11d}$$

Kets on the right-hand side of (2.11) are of the direct-product form $|m_S\rangle|m_I\rangle = |m_S\, m_I\rangle$. Given that the electronic angular momentum under consideration is half-odd-integral, if the nuclear spin is half-odd-integral, we will have two nondegenerate states corresponding to $M_F = 0$ and doubly degenerate states corresponding to $M_F = \pm 1,\ \pm 2$, etc. Since total (actual) angular momentum would then be integral, there is no requirement of degeneracy imposed by time-reversal symmetry. Degeneracy present is, however, required by axial symmetry of the system. If the nuclear spin were nonzero integral (rare-earth nuclei with nonzero integral spins are highly unstable), our system would have only doubly degenerate hyperfine levels, as required by Kramers theorem.

Neodymium has two naturally occurring isotopes with nonzero spin, ^{143}Nd and ^{145}Nd, erbium has one, ^{167}Er; in all cases $I = \frac{7}{2}$. We present calculations of spin-lattice-relaxation rates for $^{143}Nd^{3+}$ and $^{167}Er^{3+}$ in both $LaCl_3$ and LaES. Spin-Hamiltonian parameters are presented in Table III, hyperfine states and energy levels in Table IV, and hyperfine wave functions in Table V. Figure 1 contains a relative energy plot of zero-field hyperfine levels for the four salts under consideration.

III. RELAXATION IN A MULTILEVEL SYSTEM WITH DEGENERATE LEVELS

In order to treat the problem of zero-field paramagnetic relaxation realistically, it is necessary to find a concise formalism for calculating time evolution of a system which has many levels of non-negligible population. It is convenient to start with a master (Pauli) equation, which for a system with *nondegenerate levels* may be written as

$$\frac{dN_i}{dt} = \sum_j \left(-W_{i\to j} N_i + W_{j\to i} N_j\right) \ . \tag{3.1}$$

Here N_i is the population of the ith level of the paramagnetic ion; transition probabilities $W_{i\to j}$ are obtained by averaging over the appropriate lattice states. The transition probabilities may be calculated from the "golden rule,"

$$W_{i\to j} = \frac{2\pi}{\hbar}\left|\langle\beta|\, V\,|\alpha\rangle\right|^2 \rho(E) \ , \tag{3.2}$$

in which β corresponds to a final state of the ion-

TABLE III. Spin-Hamiltonian parameters [see Eq. (2.9)].

System	A(MHz) ($\pm\sigma$)	B(MHz) ($\pm\sigma$)	P(MHz) ($\pm\sigma$)
$LaCl_3$: ^{143}Nd[a]	1273.07 (± 0.30)	499.506 (± 0.010)	0.26 (± 0.15)
LaES: ^{143}Nd[a]	1139.35 (± 0.44)	595.03 (± 0.05)	1.76 (± 0.59)
$LaCl_3$: ^{167}Er[b]	−199.0 (± 0.9)	911.2 (± 0.6)	25.8
LaES: ^{167}Er[b]	−155.9 (± 3.0)	941.1 (± 3.0)	89.9 (± 9.0)

[a]Reference 1, zero-field data.
[b]Reference 3, p. 303ff.

lattice system, with the ion in state j, and α corresponds to an initial state of this system, with the ion in state i. $\rho(E)$ is the density of final states.

In the systems under consideration there are both doubly and singly degenerate levels. Writing these states in the form (2.11) with the crystal field states given in Table II, and f representing F or $F-1$, we have

$$|\langle fM_F|V|f'0\rangle|^2=|\langle f-M_F|V|f'0\rangle|^2\ , \tag{3.3a}$$

$$|\langle fM_F|V|f'M'_F\rangle|^2=|\langle f-M_F|V|f'-M'_F\rangle|^2\ , \tag{3.3b}$$

$$|\langle fM_F|V|f'-M'_F\rangle|^2=|\langle f-M_F|V|f'M'_F\rangle|^2\ , \tag{3.3c}$$

and with one minor exception,[11] either $|\langle fM_F|V|\times f'M_F\rangle|$ or $|\langle fM_F|V|f'-M_F\rangle|$ is equal to zero. If we assume that the system has been prepared symmetrically, that is, its density matrix is diagonal and that, if i and j are degenerate states, $\rho_{ii}=\rho_{jj}$, the above-mentioned properties of the pertrubation ensure that the system will evolve in a symmetrical manner. It is therefore possible to write the master equation for such a system of *degenerate levels* as

$$\frac{dg_iN_i}{dt}=\sum_j\left(-W_{i\to j}g_iN_i+W_{j\to i}g_jN_j\right)\ . \tag{3.4}$$

$W_{i\to j}$ now represents the transition probability from one state in the ith level to one state in the jth level, N_i is the population of a state in the ith level, and g_i is the degeneracy of that level. Now at thermal equilibrium, we have

$$\frac{N_i}{N_j}=\exp\left(-\frac{E_i-E_j}{kT}\right)\ , \tag{3.5}$$

so that

$$\frac{W_{j\to i}}{W_{i\to j}}=\frac{g_i}{g_j}\exp\left(-\frac{E_i-E_j}{kT}\right)\ . \tag{3.6}$$

The computation of transition rates and eigenvalues of a relaxing system is made easier if we define a symmetric matrix $\underline{T}$ proportional to the transition probability as follows:

$$W_{j\to i}=g_iT^{ij}\exp\left(-\frac{E_i-E_j}{2kT}\right), \tag{3.7a}$$

$$W_{i\to j}=g_jT^{ij}\exp\left(\frac{E_i-E_j}{2kT}\right)\ . \tag{3.7b}$$

For the systems and the temperature range with which we are concerned, $kT\gg E_i-E_j$, the dominant temperature dependence of the transition rates appears in the T^{ij}. All T^{ij} for a given relaxation mechanism have the same temperature dependence; thus the eigenvalues of $\underline{W}$ have very nearly the temperature dependence of the T^{ij}. We refer to this dependence as the characteristic or "process" temperature dependence.

Also for convenience, the population of the ith *level* is defined to be $P_i=g_iN_i$. (We will use P_{44} to denote the population of the level composed of $|44\rangle$ and $|4-4\rangle$ with similar notation for other subscripted quantities.) Equations (3.4) are cast into matrix form,

$$\frac{d\underline{P}}{dt}=\underline{W}\underline{P}\ , \tag{3.8}$$

in which $\underline{P}$ is a vector with components P_i and $\underline{W}$ is a matrix, called the *transition-rate matrix*, given by

$$W_{ij}=W_{j\to i}\ (i\neq j)\ , \tag{3.9a}$$

$$W_{ii}=-\textstyle\sum_j W_{i\to j}=-\sum_j W_{ji}\ . \tag{3.9b}$$

Note that $\underline{W}$ has negative diagonal elements and non-negative off-diagonal elements. $\underline{W}$ itself is

TABLE IV. Zero-field hyperfine energy levels (see Sec. II). $|FM_F\rangle$ is degenerate with $|F-M_F\rangle$.

Level $\lvert FM_F\rangle$	Energy (MHz) $LaCl_3$: ^{143}Nd	LaES: ^{143}Nd	$LaCl_3$: ^{167}Er	LaES: ^{167}Er
$\lvert4\pm4\rangle$	2229.69	2006.18	−167.89	356.67
$\lvert4\pm3\rangle$	1702.73	1599.00	1415.42	1741.61
$\lvert4\pm2\rangle$	1220.27	1247.12	1621.93	1613.35
$\lvert4\pm1\rangle$	838.49	922.74	1715.58	1509.51
$\lvert40\rangle$	679.44	898.42	1743.23	1471.65
$\lvert30\rangle$	−1318.58	−1483.70	−1901.42	−2292.90
$\lvert3\pm1\rangle$	−1477.10	−1576.50	−1822.23	−2150.92
$\lvert3\pm2\rangle$	−1857.33	−1820.32	−1573.96	−1715.26
$\lvert3\pm3\rangle$	−2337.19	−2154.59	−1109.76	−944.34

TABLE V. Zero-field hyperfine wave functions [see Eq. (2.11)].

M_F	$LaCl_3$: ^{143}Nd $a(M_F)$	$b(M_F)$	LaES: ^{143}Nd $a(M_F)$	$b(M_F)$	$LaCl_3$: ^{167}Er $a(M_F)$	$b(M_F)$	LaES: ^{167}Er $a(M_F)$	$b(M_F)$
4	1.0	0.0	1.0	0.0	1.0	0.0	1.0	0.0
3	0.986	0.166	0.977	0.215	0.593	0.806	0.559	0.829
2	0.956	0.294	0.933	0.360	0.649	0.760	0.632	0.775
1	0.880	0.475	0.849	0.528	0.681	0.732	0.674	0.739
0	0.707	0.707	0.707	0.707	0.707	0.707	0.707	0.707

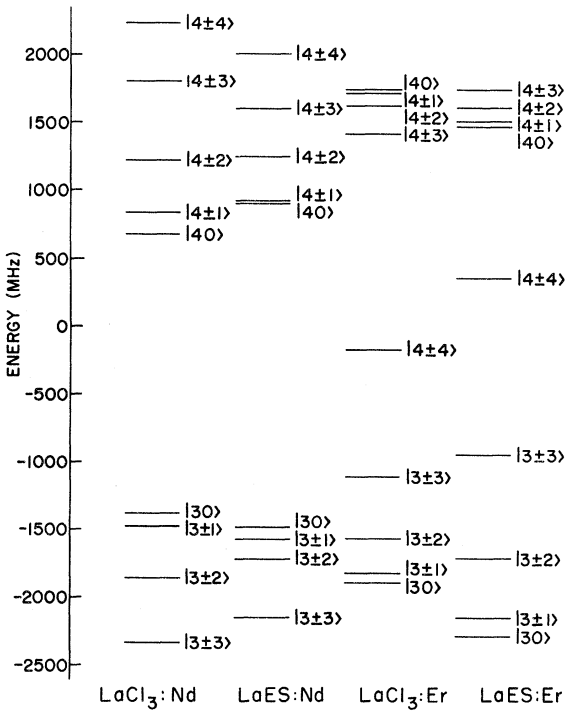

FIG. 1. Hyperfine energy levels of $^{143}Nd^{3+}$ in $LaCl_3$ and LaES and of $^{167}Er^{3+}$ in $LaCl_3$ and LaES. The levels are labeled in the $|FM_F\rangle$ representation.

not symmetric, and it turns out to be more convenient to work with the scaled symmetric (*reduced-transition-rate*) matrix $\underline{W}=\underline{U}\,\underline{W}\,\underline{U}^{-1}$. $\underline{U}$ is a diagonal matrix such that

$$U_{ii}=\frac{1}{\sqrt{g_i}}\exp\left(\frac{E_i-E_{\rm ref}}{2kT}\right), \tag{3.10}$$

$$U_{ii}^{-1}=\sqrt{g_i}\exp\left(-\frac{E_i-E_{\rm ref}}{2kT}\right), \tag{3.11}$$

in which $E_{\rm ref}$ is any convenient reference energy. Then we have

$$\tilde{W}_{ij}=(g_i\,g_j)^{1/2}T^{ij}=(\underline{U}\,\underline{W}\,\underline{U}^{-1})_{ji}\quad(i\neq j). \tag{3.12}$$

Equation (3.1) can then be rewritten to obtain the time dependence of the "transformed" population vector,

$$\frac{d\underline{U}\,\underline{P}}{dt}=\underline{U}\,\underline{W}\,\underline{U}^{-1}\,\underline{U}\,\underline{P}=\underline{U}\,\underline{W}\,\underline{P}. \tag{3.13}$$

The state of the system can be represented at any time as a linear combination of eigenvectors $\underline{X}_i$ of $\tilde{\underline{W}}$. Thus expanding the initial state of our system as

$$\underline{U}\,\underline{P}(0)=\textstyle\sum_i C_i(0)\,\underline{X}_i, \tag{3.14}$$

the state of the system at any time t is given by

$$\underline{P}(t)=\underline{U}^{-1}\textstyle\sum_i C_i(0)\,e^{-\lambda_i t}\,\underline{X}_i. \tag{3.15}$$

The nature of W_{ij} (3.6) assures that we will have one of the λ_i, say λ_1, equal to zero and the remaining λ_i all greater than zero. $\underline{U}^{-1}\underline{X}_1$ then represents the equilibrium state of the system and C_1 the total number of particles in the system. The population of a level not at equilibrium evolves toward equilibrium as a sum of exponential decays. The λ_i are referred to as relaxation rates and the λ_i^{-1} relaxation times. A system of L levels would have $L-1$ relaxation times.

The results of these relaxation calculations are presented as follows. An algebraic formula for T^{ij} is derived; from this, $\tilde{\underline{W}}$ may be computed. In discussing time evolution of systems, we present relaxation rates λ_i and corresponding eigenvectors $\underline{X}_i$. From (3.10)–(3.13) it is then possible to compute observed signal intensities as a function of time and absolute temperature (*vide infra*).

IV. ION-LATTICE INTERACTION

We express time-independent ion-lattice interactions, represented by a Hamiltonian $\mathcal{H}_{il}$, in terms of a series of products of a lattice operator times an ion operator. Invariably the harmonic approximation for lattice motion is used. One basic difficulty with this approach is that operators most natural for description of ion states (some set of operator equivalent factors operating on total $\vec{J}$ and transforming as spherical harmonics) and operators most natural for description of lattice vibrations (phonon creation and annihilation operators) have different transformation properties and are generally incompatible. Stevens derives the ion-lattice Hamiltonian as[12]

$$\mathcal{H}_{il}=\sum_{\vec{k}}|\vec{k}|\,(\hbar/2M\omega_{\vec{k}})^{1/2}(\alpha_{\vec{k}}+\alpha_{\vec{k}}^{\dagger})\,U_{\vec{k}}(J)$$
$$+\sum_{\vec{k},\vec{k}'}|\vec{k}|\,|\vec{k}'|\,(\hbar/2M\omega_{\vec{k}})^{1/2}(\hbar/2M\omega_{\vec{k}'})^{1/2}$$
$$\times(\alpha_{\vec{k}}+\alpha_{\vec{k}}^{\dagger})(\alpha_{\vec{k}'}+\alpha_{\vec{k}'}^{\dagger})\,U_{\vec{k}\,\vec{k}'}(J). \tag{4.1}$$

This equation is obtained by using a Taylor-series expansion of the crystal field potential in terms of displacements of the lattice ions from equilibrium positions, then transforming to the normal modes of the lattice. The $\alpha_{\vec{k}}$, $\alpha_{\vec{k}}^{\dagger}$ are the annihilation and creation operators for phonons of wave vector $\vec{k}$, frequency $\omega_{\vec{k}}$. The $U_{\vec{k}}$, $U_{\vec{k}\,\vec{k}'}$ have the dimensions of crystal-field-operator equivalents.

Spin-lattice-relaxation calculations typically involve two expansions. First, the ion-lattice Hamiltonian is expanded in terms of lattice normal modes. Then transition probabilities are computed using the golden rule of time-dependent perturbation theory (3.2), in which the time-evolution operator is expanded in the usual way.[13] These expansions are truncated at an appropriate point resulting in the now familiar direct, Raman, and

Orbach (resonance Raman) processes. Orbach[6,7] wrote an interaction Hamiltonian for paramagnetic ions in a crystal field (without hyperfine interaction) as

$$\mathcal{H}_{11} = \sum_{n,m} V_n^m \epsilon_{nm}(L) = \sum_{n,m} B_n^m \langle r^n \rangle \chi_n O_n^m(J) \epsilon_{nm}(L) . \tag{4.2}$$

In effect Orbach chose to work with a time-independent ion-lattice interaction as a sum of products using the linear combination of lattice modes suited to a given operator equivalent, $O_n^m(J)$. B_n^m is a "dynamic crystal field parameter," χ_n is the α, β, γ of Elliott and Stevens,[14] and $\epsilon_{nm}(L)$ appropriate lattice operators ("strain") for a given n, m. Thus Orbach limited himself to the first term of (4.1) and further set $U_{\vec{k}}(J) = \sum_{n,m} B_n^m \langle r^n \rangle O_n^m(J)$. Most importantly $\epsilon_{nm}(L)$ is replaced by an average lattice strain operator

$$\epsilon = \sum_{\vec{k}} |\vec{k}| (\hbar/2m\omega_{\vec{k}})^{1/2} (\alpha_{\vec{k}} + \alpha_{\vec{k}}^\dagger) . \tag{4.3}$$

In addition, Orbach estimated the values of B_n^m based on the static crystal field parameters.

Scott and Jeffries[9] wrote the same interaction as

$$\mathcal{H}_{11} = \epsilon \sum_{n,m} V_n^m = \epsilon \sum_{n,m} b_n^m \langle r^n \rangle \chi_n Q_n^m(J) . \tag{4.4}$$

We prefer this form, using irreducible spherical tensor operators $Q_n^m(J)$, because forthcoming approximations are then possible and a more clear physical picture obtains. For rare-earth paramagnetic ions, n is restricted to 2, 4, 6, leaving 15 constants b_n^m to be evaluated. Scott and Jeffries give plausible arguments for

$$|b_n^m \langle r^n \rangle| = |A_n^0 \langle r^n \rangle|_{\text{expt}} . \tag{4.5}$$

They further assert that contributions from different n, m are "incoherent," giving transition probabilities depending on

$$\sum_{n,m} |\langle b| \epsilon V_n^m |a\rangle|^2 \tag{4.6}$$

instead of

$$|\langle b| \epsilon \sum_{n,m} V_n^m |a\rangle|^2 . \tag{4.7}$$

Consideration of group-theoretical approaches to the ion-lattice interaction leads us to a simple physical picture for the Scott-Jeffries method. The paramagnetic ion is considered to be embedded in an isotropic elastic medium in which the static crystal field is maintained by some external agency. A spherically symmetrical charge distribution exists about the paramagnetic ion embedded in the elastic lattice. For the ion-lattice interaction the site group is then the full rotation group. The electronic operators which transform as irreducible representations of the rotation group are just the $Q_{n_1}^m(J)$. The appropriate linear combinations of lattice strains also transform as spherical harmonics $Q_{n_2}^m(L)$, and we may write ion-lattice interactions using the theory of irreducible tensors.[10] There will be no invariant products unless $n_1 = n_2$ and our Hamiltonian reduces to

$$\mathcal{H}_{11} = \sum_{n,m} C_n \langle nn\,0\,0 | n - m\, n\, m \rangle Q_n^{-m}(L) Q_n^m(J)$$

$$= \sum_{n,m} \frac{C_n}{(2n+1)^{1/2}} (-1)^n Q_n^{-m}(L) Q_n^m(J) . \tag{4.8}$$

$\langle j_1 j_2 j\, m | j_1 m_1 j_2 m_2 \rangle$ is, as before, a Clebsch-Gordan coefficient. In this approximation all b_n^m should be equal for a given n, and the orthogonality of the Q_n^m is used to pass from a "coherent" square of the sum to an "incoherent" sum of squares.

In the calculations presented here we shall use the Scott-Jeffries Hamiltonian (4.4) neglecting the effects of lattice vibrations on the nuclear state. While it is quite certain that this accounts for a major part of ion-lattice interactions, we take note here that nuclear relaxation will also occur. We point out that a more general, though still approximate, treatment might involve an interaction Hamiltonian expressed as a sum of invariant products of the set $Q_n^m(L)$ ($n = 1, \ldots, 8$), $Q_n^m(I)$ ($n = 0, 1, 2$), and $Q_n^m(J)$ ($n = 0, 2, 4, 6$). This more general, comprehensive approach, employing irreducible-tensor-operator products, is currently being pursued in conjunction with a density-matrix description of the ion-lattice system.

V. RELAXATION PROCESSES AT ZERO FIELD

A. Direct Process

We first calculate the probability for an ion to undergo the transition from state $|j\rangle$ to a lower-lying state $|i\rangle$ accompanied by emission of a single phonon of the required energy for energy conservation (direct process):

$$W_{j\to i}^{\text{direct}} = (2\pi/\hbar) |\langle j, N| \mathcal{H}_{11} |i, N+1\rangle|^2 \times \delta(E(j,N) - E(i,N+1)) . \tag{5.1}$$

This expression is averaged over all normal modes of the lattice. Using a Debye model for lattice vibrations,

$$W_{j\to i}^{\text{direct}} = \frac{3}{2\pi\rho v^5 \hbar} \left(\frac{E_j - E_i}{\hbar}\right)^3 (N+1) V(j,i) , \tag{5.2}$$

$$W_{i\to j}^{\text{direct}} = \frac{3}{2\pi\rho v^5 \hbar} \left(\frac{E_j - E_i}{\hbar}\right)^3 N V(j,i) . \tag{5.3}$$

In the above equations, we have

$$V(j,i) = \sum_{n,m} |\langle j| V_n^m |i\rangle|^2 ; \tag{5.4}$$

ρ is the density of the crystal (3.84 g/cm^3 for $LaCl_3$,[15] 1.8 g/cm^3 for LaES[9]); v is the velocity of

sound in the crystal (assumed to be 2×10^5 cm/sec in both cases)[15,9]; N is the occupation number for a phonon mode of energy $(E_j - E_i)$ given by

$$N = (e^{(E_j - E_i)/kT} - 1)^{-1} ; \tag{5.5}$$

and V_n^m is defined by (4.4).

$\langle i|Q_n^m(J)|j\rangle$ vanishes when $|i\rangle$ and $|j\rangle$ are eigenstates of the spin Hamiltonian (2.9). This is generally true for a state derived from an electronic Kramers doublet, even though the ion as a whole (electronic plus nuclear coordinates) may not be a Kramers system. Thus, zeroth-order hyperfine states apparently have no direct relaxation process available to them. However, the term $\mathcal{H}_{hf} = a(\vec{I}\cdot\vec{J})$ in (2.1) admixes excited electronic states into these hyperfine levels as follows:

$$|FM_F\rangle' = |FM_F\rangle - \sum_{n,m_I}\left(\frac{|(\tfrac{1}{2})^n m_I\rangle\langle(\tfrac{1}{2})^n m_I|a\vec{I}\cdot\vec{J}|FM_F\rangle}{\Delta_n} + \frac{|(-\tfrac{1}{2})^n m_I\rangle\langle(-\tfrac{1}{2})^n m_I|a\vec{I}\cdot\vec{J}|FM_F\rangle}{\Delta_n}\right) , \tag{5.6}$$

in which Δ_n is the energy difference between the ground and excited Kramers doublets neglecting the energy due to hyperfine splitting of these states. There are excited electronic states mixed in by the J_z part of the perturbation and by the $J_\pm$ parts of the perturbation but not by both. Clearly the magnitude of the direct process will depend on the energies of the excited electronic states. The favored direct-process transitions will be different depending on which of the operators connects the ground doublet to the low-lying excited state.

For an excited electronic state $|\tfrac{1}{2}^z\rangle$ such that $\langle\tfrac{1}{2}^z|J_z|\tfrac{1}{2}\rangle \neq 0$, we have

$$\langle\tfrac{1}{2}^z|J_z|\tfrac{1}{2}\rangle = \langle\tfrac{1}{2}|J_z|\tfrac{1}{2}^z\rangle = -\langle-\tfrac{1}{2}^z|J_z|-\tfrac{1}{2}\rangle , \tag{5.7}$$

$$\langle\tfrac{1}{2}^z|J_z|-\tfrac{1}{2}\rangle = 0 . \tag{5.8}$$

Equations (5.6)–(5.8) give rise to a $\Delta M_F = 0, \pm1$ selection rule for a direct process between ground-state hyperfine levels when J_z is the operator coupling ground and excited states.

We make use of the following properties of the two sets of Kramers doublets $|\pm\tfrac{1}{2}\rangle$ and $|\tfrac{1}{2}^z\rangle$ in order to calculate $V(j, i)$ (5.4):

$$\langle\pm\tfrac{1}{2}|Q_n^m|\pm\tfrac{1}{2}^z\rangle = \langle\mp\tfrac{1}{2}^z|Q_n^m|\mp\tfrac{1}{2}\rangle , \tag{5.9}$$

$$\langle\pm\tfrac{1}{2}|Q_n^m|\mp\tfrac{1}{2}^z\rangle = -\langle\pm\tfrac{1}{2}^z|Q_n^m|\mp\tfrac{1}{2}\rangle . \tag{5.10}$$

Now consider an excited state $|\tfrac{1}{2}^+\rangle$ such that $\langle\tfrac{1}{2}^+|J_+|\tfrac{1}{2}\rangle \neq 0$. The following property of the matrix elements is useful in constructing the new ground state:

$$\langle-\tfrac{1}{2}^+|J_-|-\tfrac{1}{2}\rangle = \langle\tfrac{1}{2}^+|J_+|\tfrac{1}{2}\rangle . \tag{5.11}$$

$\Delta M_F = 0$ transitions are not allowed by $J_\pm$ admixtures, while $\Delta M_F = \pm1, \pm2$ transitions are. In computing the transition probabilities associated with wave functions of this form, we use the identities

$$\langle\pm\tfrac{1}{2}|Q_n^m|\pm\tfrac{1}{2}^+\rangle = -\langle\mp\tfrac{1}{2}^+|Q_n^m|\mp\tfrac{1}{2}\rangle , \tag{5.12}$$

$$\langle\pm\tfrac{1}{2}|Q_n^m|\mp\tfrac{1}{2}^+\rangle = \langle\pm\tfrac{1}{2}^+|Q_n^m|\mp\tfrac{1}{2}\rangle . \tag{5.13}$$

From (3.7) and (5.2), we calculate T^{ij}_{direct}:

$$T^{ij}_{\text{direct}} = \frac{3}{2\pi\rho v^5\hbar}\left(\frac{E_j - E_i}{\hbar}\right)^3 N\exp\left(\frac{E_j - E_i}{kT}\right) V(j, i) , \tag{5.14}$$

and since

$$N\exp\left(\frac{E_j - E_i}{2kT}\right) \approx \frac{2kT}{E_j - E_i} , \tag{5.15}$$

we have

$$T^{ij} \approx \frac{3}{2\pi\rho v^5\hbar^2}\left(\frac{E_j - E_i}{\hbar}\right)^2 (2kT)\, V(j, i) . \tag{5.16}$$

Direct-process transition rates increase approximately linearly with temperature as in the more usual high-field case. The relative size of transition probabilities depends on a number of factors, hyperfine splitting between the two levels, which excited state lies lowest, and so on. The direct process is fastest for LaES:Er but even here the shortest relaxation time is greater than 1 sec. Relaxation rates and associated eigenvectors of the scaled or reduced transition rate matrix $\underline{\tilde{W}}$ are given in Table VI for LaES:Er.

As pointed out in Sec. III, the quantities of experimental interest are $\underline{W}$ and $\underline{P}(t)$, not $\underline{\tilde{W}}$ and $\underline{\tilde{X}}$. It turns out, however, to be so much more convenient and illuminating to present and work with $\underline{\tilde{W}}$ and $\underline{X}$ that we use these two quantities until experimental observables are discussed in Sec. VI. In the temperature range considered here (kT greater than the hyperfine splitting of the ground state), T^{ij} displays the characteristic temperature dependence of the direct-process relaxation rates λ_j.

B. Raman Process

The direct process is seen to be slow even at the lowest temperatures. We now go to second order in perturbation theory, considering two-phonon processes for which the *difference* in phonon energies equals the energy separation of the levels involved. The perturbation is then, in effect,

$$V_{eff} = \sum_{\substack{n,m \\ n',m' \\ t}} \frac{V_n^m |t\rangle\langle t| V_{n'}^{m'}}{E_0 - E_t} , \tag{5.17}$$

in which the summation runs over all intermediate states and $E_0 - E_t$ is the energy difference between initial and intermediate states of the combined ion-lattice system. The summation is taken over all hyperfine levels derived from excited Kramers doublets. For the moment, an actual ion transition to an excited level characterized by a vanishing denominator in (5.17) is excluded; a *Raman* relaxation process thus obtains. Following Orbach's derivation, the Raman relaxation transition rate between initial ($|i\rangle$) and final ($|j\rangle$) states of the ion is

$$T_{\text{Raman}}^{ij} = \frac{9\times 6!}{8\pi^3\rho^2 v^{10}} V_R(i,j) \left(\frac{kT}{\hbar}\right)^7 , \tag{5.18}$$

in which

$$V_R(i,j) = \sum_{\substack{n,m \\ n',m'}} \left| \sum_t \frac{\langle i| V_n^m |t\rangle\langle t| V_{n'}^{m'} |j\rangle}{\Delta_t} \right|^2 . \tag{5.19}$$

It should be noted that use of the second term in the ion-lattice interaction (4.1) in first-order perturbation theory also leads to a Raman process for which the transition probability increases as T^7,

$$T^{ij} = \frac{9\times 6!}{8\pi^3\rho^2 v^{10}} \left(\frac{kT}{\hbar}\right)^7 \sum_{n,m} |\langle i| V_n^m |j\rangle|^2 . \tag{5.20}$$

This process is not considered here because, as explained for the direct process, $|\langle i| V_n^m |j\rangle|^2$ vanishes in first order and has a small nonzero value only for hyperfine admixtures of excited states. It is thus safely neglected compared to (5.19) when dealing with Kramers-conjugate *electronic* states and the restricted ion-lattice interaction (4.4).

At this point it seems appropriate to contrast zero-field Raman hyperfine relaxation for electronic Kramers doublets with Raman relaxation for both high-field Kramers doublets and non-Kramers electronic ions. The transition probability for a Raman process depends on sums of the form

$$\sum_t \frac{\langle a|\mathcal{H}_{11}|t\rangle\langle t|\mathcal{H}_{11}|b\rangle}{E_a - E_t} ,$$

in which a, t, b are states of the combined ion-lattice system. In high field, relaxation between zero-field Kramers-conjugate degenerate states has a T^9 temperature dependence due to a near cancellation (the "Van Vleck cancellation") of terms in the above sum. However, at zero field in the presence of strong hyperfine interaction, we actually have a non-Kramers situation in that relaxation occurs between states which are *not* Kramers conjugates of one another. Therefore, no Van Vleck cancellation ensues, and a T^7 temperature dependence, characteristic of a non-Kramers system, results.

The sum in (5.19) runs over the states in excited hyperfine multiplets. States in the nth hyperfine multiplet would be of the form

$$|F^n M_F\rangle = a^n(M_F)\left|\tfrac{1}{2}^n M_F - \tfrac{1}{2}\right\rangle + b^n(M_F)\left|-\tfrac{1}{2}^n M_F + \tfrac{1}{2}\right\rangle , \tag{5.21}$$

$$|(F-1)^n M_F\rangle = b^n(M_F)\left|\tfrac{1}{2}^n M_F - \tfrac{1}{2}\right\rangle - a^n(M_F)\left|-\tfrac{1}{2}^n M_F + \tfrac{1}{2}\right\rangle , \tag{5.22}$$

in analogy with (2.11). Our assumption that the ion-lattice interaction affects only electronic states requires a $\Delta M_F = 0, \pm 1$ selection rule for each matrix element in (5.19). $\Delta M_F = \pm 2$ transitions are also not allowed because

$$\langle f M_F| V_n^m |F^t M_F \pm 1\rangle\langle F^t M_F \pm 1| V_{n'}^{m'} |f' M_F \pm 2\rangle + \langle f M_F| V_n^m |(F-1)^t M_F \pm 1\rangle \times \langle (F-1)^t M_F \pm 1| V_{n'}^{m'} |f' M_F \pm 2\rangle = 0 , \tag{5.23}$$

in which f and f' represent either F or $F-1$. We are, therefore, left with $\Delta M_F = 0, \pm 1$ transitions. Moreover, if hyperfine splitting of the excited state is neglected in comparison with crystal field split-

TABLE VI. Relaxation rates and eigenvectors of $\underline{\tilde{W}}$ (direct process only) for LaES:Er at 4.2 K (see Sec. III). The components of $\underline{X}_k$ are in the X_{kFM_F} notation.

k	Rate λ_k(sec^{-1})	Eigenvector components X_{k44}	X_{k43}	X_{k42}	X_{k41}	X_{k40}	X_{k30}	X_{k31}	X_{k32}	X_{k33}
1	0.0	0.3007	0.2983	0.2985	0.2987	0.4225	0.4317	0.3050	0.3043	0.3029
2	0.085	−0.7996	−0.1000	0.2115	0.1701	−0.1534	0.3868	0.0372	0.1439	0.2858
3	0.103	0.5038	0.4476	−0.2466	−0.0562	0.4655	−0.3791	0.1785	0.2430	−0.1750
4	0.167	0.0775	0.8086	0.0316	−0.0212	−0.5139	0.0233	0.0246	−0.2674	0.0439
5	0.179	0.0588	−0.0555	−0.2296	0.0704	−0.0339	−0.5403	0.0038	−0.0169	0.8553
6	0.514	0.0394	−0.1682	−0.1852	0.6102	−0.1859	−0.1767	0.6386	−0.2029	−0.2208
7	0.585	0.0184	−0.0639	0.5275	−0.4543	0.2123	−0.2345	0.4329	−0.4703	0.0473
8	0.723	−0.0701	−0.0461	0.5671	0.0821	−0.3853	−0.3899	0.0274	0.5997	−0.0615
9	0.887	0.0102	0.0960	0.3428	0.5364	0.2965	−0.2806	−0.5265	−0.3659	−0.0875

ting between ground and excited states in determining Δ_t, the coefficients in (5.2) combine in such a way as to not appear explicitly in $V_R(i,j)$. This fact is summarized below as follows:

$$V_R(F\,M_F, F-1\,M_F) = a^2(M_F)b^2(M_F)\delta\,,$$

$$V_R(F\,M_F, F\,M_F-1) = a^2(M_F)b^2(M_F-1)\sigma\,,$$

$$V_R(F-1\,M_F, F-1\,M_F+1) = a^2(M_F)b^2(M_F+1)\sigma, \quad (5.24)$$

$$V_R(F\,M_F, F-1\,M_F+1) = b^2(M_F)b^2(M_F+1)\sigma\,,$$

$$V_R(F\,M_F, F-1\,M_F-1) = a^2(M_F)a^2(M_F-1)\sigma\,,$$

in which

$$\delta = \sum_{\substack{n,m\\ n',m'}} \Big| \sum_t \frac{1}{\Delta_t} \big(\langle \tfrac{1}{2}| V_n^m | -\tfrac{1}{2}t\rangle\langle -\tfrac{1}{2}t | V_{n'}^{m'} | \tfrac{1}{2}\rangle + \langle \tfrac{1}{2}| V_n^m | \tfrac{1}{2}t\rangle \langle \tfrac{1}{2}t | V_{n'}^{m'} | \tfrac{1}{2}\rangle - \langle -\tfrac{1}{2}| V_n^m | -\tfrac{1}{2}t\rangle\langle -\tfrac{1}{2}t | V_{n'}^{m'} | -\tfrac{1}{2}\rangle - \langle -\tfrac{1}{2}| V_n^m | \tfrac{1}{2}t\rangle \langle \tfrac{1}{2}t | V_{n'}^{m'} | -\tfrac{1}{2}\rangle\big)\Big|^2 \quad (5.25)$$

and

$$\sigma = \sum_{\substack{n,m\\ n',m'}} \Big| \sum_t \frac{1}{\Delta_t} \big(\langle \tfrac{1}{2}| V_n^m | \tfrac{1}{2}t\rangle\langle \tfrac{1}{2}t | V_{n'}^{m'} | -\tfrac{1}{2}\rangle + \langle \tfrac{1}{2} | V_n^m | -\tfrac{1}{2}t\rangle\langle -\tfrac{1}{2}t | V_{n'}^{m'} | -\tfrac{1}{2}\rangle\big)\Big|^2 . \quad (5.26)$$

The values of δ and σ are listed in Table VII.

Raman relaxation, as we have represented it by (5.19), is greatest in the LaES:Er system and least in the $LaCl_3$:Er system. Much of this difference in rates between a $LaCl_3$ system and a LaES system stems from a difference in densities.

C. Orbach Process

We now consider the possibility of an ion absorbing a phonon of energy Δ_t followed by transition to one of the ground hyperfine states via emission of an appropriate phonon. This "resonance Raman" process is usually referred to in the literature as the Orbach process, and corresponds to the denominator $E_0 - E_t$ vanishing in the effective Hamiltonian (5.17). In order for this type of a process to occur, there must be real phonons of energy equal to or greater than the ion energy difference Δ_t; that is, $\hbar\omega \geq \Delta_t$. Only for $LaCl_3$:Er and LaES:Er, of the systems we consider, are there low-lying excited electronic Kramers doublets $|\pm\tfrac{1}{2}^n\rangle$ with energy less than the Debye energy of the crystal. ($\Theta_D = 149.5$ K for $LaCl_3$,[16] $\Theta_D \approx 60$ K for LaES.[9]) In what follows we consider only the lowest-lying excited electronic Kramers doublet.[17] To calculate Orbach relaxation rates we must, as demonstrated by Orbach,[7] find the linewidth of the excited state involved. According to Heitler,[18] the linewidth of a level t is proportional to the sum of transition probabilities from t to all lower levels. In what follows, linewidths of states in the lowest hyperfine multiplet are ignored, while linewidths of states in the first excited hyperfine multiplet are assumed to be determined solely by (direct-process) decay rates to states in the lowest hyperfine split multiplet. Then the linewidth Γ_t of a given excited state t is found to be (in cm^{-1})

$$\Gamma_t = \frac{3}{2\pi\rho v^5}\left(\frac{\Delta_t}{\hbar}\right)^3 \sum_{\substack{n,m\\ M_F}} \big(|\langle F\,M_F | V_n^m | t\rangle|^2 + |\langle F-1\,M_F | V_n^m | t\rangle|^2\big)(N+1)\,, \quad (5.27)$$

neglecting hyperfine splitting energy in comparison to crystal field splitting energy in evaluation of Δ_t. It turns out that the lowest-excited-state electronic wave functions for Er^{3+} in both $LaCl_3$ and LaES satisfy $\langle \tfrac{1}{2}^1 | J_+ | -\tfrac{1}{2}^1\rangle = 0$ (see Table II) so that hyperfine wave functions for the first excited electronic level are simply direct products of electronic and nuclear wave functions $|m_S m_I\rangle$ degenerate with $|-m_S - m_I\rangle$. Therefore, within the approximation described, all hyperfine states in an excited multiplet have the same linewidth. For $LaCl_3$:Er we have

$$\sum_{\substack{n,m\\ t}} |\langle i | V_n^m | t\rangle|^2 = 2.904\times 10^3\ \text{cm}^{-2}\,, \quad (5.28)$$

while for LaES:Er we have

$$\sum_{\substack{n,m\\ t}} |\langle i | V_n^m | t\rangle|^2 = 4.754\times 10^3\ \text{cm}^{-2}\,. \quad (5.29)$$

Equation (5.27) gives the energy width of the states; the frequency width is obtained from

$$\Delta\nu = \Gamma_t / h\,,$$

and substitution of appropriate values leads to

$$\Delta\nu(LaCl_3:Er) = 2.447\times 10^9\ \text{Hz}\,,$$

$$\Delta\nu(LaES:Er) = 13.36\times 10^9\ \text{Hz}\,.$$

The linewidths thus calculated seem large (of the order of the hyperfine splitting of the excited-state multiplet), although experimental linewidths are not available. It seems probable that (5.27) would be subject to considerable inaccuracy in the factor

TABLE VII. Values of δ and σ for the Raman process [see Eqs. (5.25) and (5.26)].

	$LaCl_3$: ^{143}Nd	LaES: ^{143}Nd	$LaCl_3$: ^{167}Er	LaES: ^{167}Er
$\delta(10^4\ \text{cm}^{-2})$	7.28	2.26	1.51	3.15
$\sigma(10^4\ \text{cm}^{-2})$	3.02	1.35	1.00	1.88

$$\frac{1}{v^5}\left(\frac{\Delta_t}{\hbar}\right)^3$$

as the density of phonon states is not likely to resemble a Debye model near the edge of the Brillouin zone.

Using this linewidth in the denominator of V_{eff} (5.17) and proceeding with the usual Raman-type evaluation, the transformed symmetric relaxation-rate matrix for individual states i and j is given by

$$T^{ij}=\frac{3}{2\pi\rho v^5\hbar}\left(\frac{\Delta}{\hbar}\right)^3(e^{\Delta/kT}-1)^{-1} \times \sum_{\substack{t,n,m\\ n,n}} \frac{|\langle i|V_n^m|t\rangle\langle t|V_n^{m'}|j\rangle|^2}{\Gamma_t} . \quad (5.30)$$

VI. GENERAL DISCUSSION AND RELATIVE STRENGTH OF RELAXATION MECHANISMS

Temperature dependences of the transition probabilities for zero-field paramagnetic relaxation are approximately (in the low-temperature range)

$$W_{\text{direct}}\propto T , \quad W_{\text{Raman}}\propto T^7 , \quad W_{\text{Orbach}}\propto e^{-\Delta/kT} .$$

At 1 K, direct-process transition probabilities are an order of magnitude smaller than those for Raman processes; at higher temperatures the direct process plays a negligible part in relaxation. In the 2–3-K range the Orbach process becomes competitive with the Raman process. To calculate the actual relaxation behavior of our systems, we have assumed

$$(W_{ij})_{\text{total}}=(W_{ij})_{\text{direct}}+(W_{ij})_{\text{Raman}}+(W_{ij})_{\text{Orbach}} , \quad (6.1)$$

in which direct processes make a negligible contribution. Diagonalizing the corresponding $\underline{\tilde{W}}$ gives relaxation rates λ_k and associated eigenvectors. To illustrate these results, we present in Table VIII relaxation rates and eigenvectors for the systems studied at 4.2 K. The following features of these data are noteworthy. The fastest relaxation times correspond approximately to relaxation occurring between a single pair of levels or a simple combination of levels. In $LaCl_3$:Nd

$|40\rangle\rightarrow|30\rangle$, $|4\pm1\rangle\rightarrow|3\pm1\rangle$,

$|4\pm3\rangle$ and $|4\pm2\rangle\rightarrow|3\pm2\rangle$, $|4\pm4\rangle\rightarrow|3\pm3\rangle$

transitions occur approximately independently of other levels. In LaES:Nd

$|40\rangle\rightarrow|30\rangle$, $|4\pm1\rangle\rightarrow|3\pm1\rangle$,

$|4\pm3\rangle$ and $|4\pm2\rangle\rightarrow|3\pm2\rangle$, $|4\pm4\rangle\rightarrow|3\pm3\rangle$

transitions evolve as approximately independent couples. In both Er systems the same is true of transitions

$|40\rangle\rightarrow|30\rangle$, $|4\pm1\rangle\rightarrow|3\pm1\rangle$,

$|4\pm2\rangle\rightarrow|3\pm2\rangle$, $|4\pm3\rangle\rightarrow|3\pm3\rangle$.

General characteristics of the decays can be understood by examining the hyperfine wave functions and remembering the underlying assumption that ion-lattice interaction affects electronic states only. Also, in the Er systems, Orbach and Raman processes, considered singly, favor the same decay pathways.

It is not strictly possible to break up relaxation rates in Er systems into Raman and Orbach components, because eigenvectors of $\underline{\tilde{W}}_{\text{Raman}}$ and $\underline{\tilde{W}}_{\text{Orbach}}$ are not identical. They are, however, quite similar and therefore, we present in Fig. 2 the fastest relaxation rate for Raman, Orbach, and combined $\underline{\tilde{W}}$ over the temperature range 2–10 K. Other relaxation rates behave similarly.

Consider now possible experimental studies of relaxation in these systems. The paramagnetic ions absorb microwave radiation with the selection rule $\Delta M_F=0, \pm1$. One method of studying the relaxation would be to saturate the transition between two hyperfine levels, followed by a sharp attenuation of incident power. Return of the system to equilibrium is followed by observing reestablishment of the signal intensity at what is called "monitoring power levels" ($\sim10^{-7}$–10^{-9} W).

For a system in its equilibrium state, level populations are given by

$$P_i^{eq}=(\text{const})g_ie^{-E_i/kT} . \quad (6.2)$$

The constant is selected to fit the number of ions in the crystal. For all our calculations we have normalized such that

$$\textstyle\sum_i P_i=1 . \quad (6.3)$$

Now suppose the transition between levels i and j is saturated so quickly that no other levels have their populations changed. The level-population vector $\underline{P}$ after such a pulse would be $\underline{P}^{sp}$ (for *short pulse*) with

$$P_i^{sp}=\left(\frac{P_i^{eq}+P_j^{eq}}{g_i+g_j}\right)g_i , \quad (6.4a)$$

$$P_j^{sp}=\left(\frac{P_i^{eq}+P_j^{eq}}{g_i+g_j}\right)g_j , \quad (6.4b)$$

$$P_k^{sp}=P_k^{eq} \quad (k\neq i \text{ or } j) . \quad (6.4c)$$

It can be easily verified that (6.4) satisfies convention (6.3) as to the number of particles in the crystal.

Another experimental situation which is easily treated is that of a saturating pulse applied to the i, j transition sufficiently long that a steady state of the system is reached, while lattice temperature

is maintained. A steady-state level-population vector $\underline{P}^{lp}$ (*long pulse*) for the system is then characterized by

$$\frac{dP_i^{lp}}{dt}=0 \quad (\text{all } i)\,. \tag{6.5}$$

For levels other than those saturated directly with microwave radiation, we assume relaxation equations still apply,

$$\frac{dP_k^{lp}}{dt}=\sum_l W_{kl}P_l=0 \quad (k\neq i \text{ or } j); \tag{6.6a}$$

levels saturated obey equations

$$P_i^{lp}=(\text{const})g_i\,, \tag{6.6b}$$

$$P_j^{lp}=(\text{const})g_j\,, \tag{6.6c}$$

in which the constant is chosen to satisfy (6.3). Equations (6.6) form a set of simultaneous linear equations which may be solved for the components of $\underline{P}^{lp}$.

The state of the system after the saturating power has been turned off is taken as the initial state $\underline{P}^{init}=\underline{P}(0)$. Using the methods of Sec. III [especially (3.14) and (3.15)], we can write

$$\underline{P}(0)=\underline{P}^{init}=\underline{U}^{-1}\textstyle\sum_l C_l\underline{X}_l\,, \tag{6.7}$$

TABLE VIII. Relaxation rates and eigenvectors of $\underline{\tilde{W}}$ (Raman and Orbach processes) for (a) $LaCl_3$: ^{143}Nd, (b) LaES: ^{143}Nd, (c) $LaCl_3$: ^{167}Er, and (d) LaES: ^{167}Er at 4.2 K (see Sec. III). The components of $\underline{X}_k$ are in the X_{kFM_F} notation.

k	Rate $\lambda_k(\text{sec}^{-1})$	X_{k44}	X_{k43}	X_{k42}	X_{k41}	X_{k40}	X_{k30}	X_{k31}	X_{k32}	X_{k33}
					Eigenvector components					
					(a) $LaCl_3$: ^{143}Nd (Raman process)					
1	0	0.3490	0.3501	0.3511	0.3518	0.2497	0.2512	0.3565	0.3573	0.3582
2	28	−0.5924	−0.0177	0.2131	0.3011	0.2302	0.2315	0.2787	0.0598	−0.0570
3	115	−0.2162	0.5945	0.0843	0.2814	−0.2847	−0.2806	−0.1596	0.5462	−0.1631
4	341	0.0433	−0.3205	0.6241	−0.0367	−0.4232	−0.4268	0.3691	−0.0841	0.0063
5	627	0.3864	−0.3604	0.3416	−0.3306	0.2329	0.2368	−0.3412	0.3552	−0.3770
6	643	−0.5700	−0.2031	0.2894	−0.2505	0.1636	0.1660	−0.2310	0.1081	0.6070
7	707	−0.0664	−0.4997	−0.4190	0.2830	−0.1388	−0.1411	0.1350	0.6505	0.0983
8	893	−0.0002	−0.0134	−0.2422	−0.6729	0.1390	0.1439	0.6678	0.0486	0.0007
9	1068	0.0000	0.0000	0.0000	0.0029	−0.7105	0.7038	−0.0008	0.0000	0.0000
					(b) LaES: ^{143}Nd (Raman process)					
1	0	0.3495	0.3503	0.3510	0.3515	0.2487	0.2521	0.3567	0.3572	0.3579
2	72	−0.5877	−0.0442	0.2047	0.3115	0.2414	0.2449	0.2848	0.0453	−0.5589
3	275	−0.2423	0.5797	0.1269	−0.2720	−0.2912	−0.2959	−0.1385	0.5402	−0.1784
4	731	0.0543	−0.3489	0.6136	−0.0270	−0.4068	−0.4165	0.3850	−0.1044	0.0098
5	1273	0.3943	−0.3600	0.3357	−0.3213	0.2239	0.2363	−0.3402	0.3578	−0.3864
6	1300	−0.5574	−0.2140	0.2981	−0.2549	0.1637	0.1734	−0.2348	0.0143	0.6057
7	1393	−0.0684	−0.4919	−0.4210	0.2894	−0.1386	−0.1493	0.1212	0.6517	0.1073
8	1582	−0.0003	−0.0164	−0.2521	−0.6727	0.1290	0.1562	0.6623	0.0633	0.0012
9	1704	0.0000	0.0000	0.0000	0.0170	−0.7189	0.6948	−0.0066	0.0000	0.0000
					(c) $LaCl_3$: ^{167}Er (Raman and Orbach processes)					
1	0	0.3539	0.3507	0.3503	0.3501	0.2475	0.2527	0.3572	0.3567	0.3558
2	45	0.5087	0.3866	0.0184	−0.3397	−0.3438	−0.3521	−0.3637	−0.0332	0.3169
3	153	−0.4945	−0.0930	0.4886	0.0083	−0.3428	−0.3548	−0.0403	0.4967	0.1272
4	265	−0.4652	0.2349	0.0530	−0.3588	0.3458	0.3699	−0.3293	−0.1094	0.4690
5	316	−0.3416	0.3325	−0.3362	0.3387	−0.2401	0.2702	0.3800	0.3733	0.3615
6	372	−0.1954	0.7248	−0.1400	−0.0004	0.0167	0.0340	−0.0907	0.2570	−0.5841
7	381	−0.0133	0.1667	0.6937	−0.1306	0.0067	−0.0456	0.1874	−0.6097	−0.2546
8	384	0.0001	−0.0044	−0.1470	−0.7030	0.0791	−0.1010	0.6571	0.1893	0.0079
9	384	0.0000	0.0000	0.0035	−0.0850	−0.7206	0.6804	0.1026	−0.0050	0.0001
					(d) LaES: ^{167}Er (Raman and Orbach processes)					
1	0	0.3528	0.3500	0.3503	0.3505	0.2479	0.2533	0.3579	0.3570	0.3554
2	257	0.5126	0.3937	0.0197	−0.3372	−0.3410	−0.3493	−0.3636	−0.0401	0.3098
3	871	−0.4924	−0.1010	0.4887	0.0043	−0.3419	−0.3535	−0.0492	0.4924	0.1477
4	1533	−0.4582	0.2358	0.0467	−0.3607	0.3510	0.3718	−0.3277	−0.1158	0.4689
5	1835	−0.3427	0.3368	−0.3413	0.3441	−0.2440	−0.2658	0.3741	−0.3683	0.3584
6	2300	−0.2068	0.7254	−0.0957	−0.0141	0.0187	0.0266	−0.0767	0.2407	−0.5973
7	2408	−0.0119	0.1305	0.7052	−0.0935	−0.0078	−0.0342	0.1671	−0.6299	−0.2253
8	2442	0.0001	−0.0030	−0.1137	−0.7091	0.0437	−0.0796	0.6718	0.1570	0.0062
9	2450	0.0000	0.0000	0.0007	−0.0564	−0.7213	0.6868	0.0691	−0.0010	0.0000

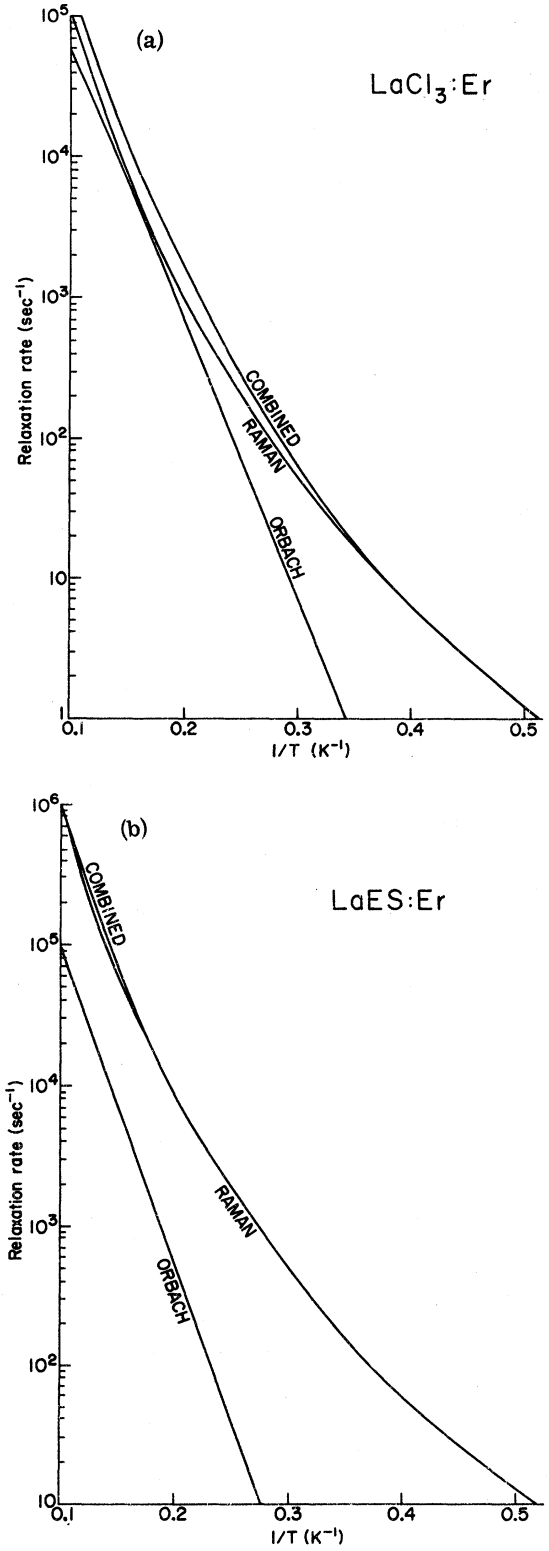

FIG. 2. Contributions of the Raman and Orbach processes to the fastest relaxation rate (λ_9 of Table VIII, corresponding to approximately a $|3\,0\rangle - |4\,0\rangle$ transition) in (a) $LaCl_3$:Er and (b) LaES:Er. Other relaxation rates behave similarly.

$$\underline{P}(t) = \underline{U}^{-1}\textstyle\sum_i C_i e^{-\lambda_i t}\underline{X}_i\,, \tag{6.8}$$

which gives us the level populations P_i as a function of time.

In a pulse-saturation experiment the recovered signal intensity will be proportional to

$$P_i/g_i - P_j/g_j\,. \tag{6.9}$$

Upon inspection of (6.8) we see that this can be written as a sum of exponentials

$$\frac{P_i}{g_i} - \frac{P_j}{g_j} = \sum_i C_i e^{-\lambda_i t}\left(\frac{U_{ii}^{-1}X_{1i}}{g_i} - \frac{U_{ji}^{-1}X_{1j}}{g_j}\right)$$

$$= \textstyle\sum_i C_i'(ij)e^{-\lambda_i t}\,, \tag{6.10}$$

in which X_{ji} is the ith component of the lth eigenvector of $\underline{W}$. The coefficients $C_i'(ij)$ must sum to zero since at $t=0$ the left-hand side of (6.10) is zero by assumption. At long times the right-hand side of (6.10) approaches $C_i'(ij)$ the equilibrium population difference given by the appropriate Boltzmann factors.

In Tables IX and X we present calculated results (6.10) for long and short saturating pulses applied to several hyperfine transitions in the $LaCl_3$: Nd^{+3} system at 4.2 K. Both $\Delta F = 1$ transitions (which occur in the microwave region, $\nu > 1$ GHz) and $\Delta F = 0$ transitions (which occur at lower frequencies, $\nu > 10$ MHz) are included. We have plotted the quantity (6.9) in Fig. 3 as a function of time for the recovery from both long and short saturating pulses. In Figs. 4 and 5 we have plotted

$$\log\left[\left(\frac{P_i}{g_i} - \frac{P_j}{g_j}\right)_{eq} - \left(\frac{P_i}{g_i} - \frac{P_j}{g_j}\right)_t\right], \tag{6.11}$$

which is the logarithm of the deviation of the signal intensity from the thermal equilibrium value. On such a plot a single-exponential decay appears as a straight line and multiexponential behavior is quite obvious. This plot is modeled after Fig. 4 of Ref. 9.

Examining the results, it is clear that the $|4\,0\rangle \rightarrow |3\,0\rangle$ transition has some unique properties. For one, identical states result for long and short saturating pulses applied to the $|4\,0\rangle \rightarrow |3\,0\rangle$ transition. This can be understood by observing that, except for direct processes which have been neglected, probability of transitions between $|4\,0\rangle$ and any other level is the same as that for $|3\,0\rangle$ and any other level. This is a direct consequence of the character of the wave function. Specifically,

$$|4\,0\rangle = (1/\sqrt{2})\left(\left|\tfrac{1}{2} - \tfrac{1}{2}\right\rangle + \left|-\tfrac{1}{2}\,\tfrac{1}{2}\right\rangle\right),$$

$$|3\,0\rangle = (1/\sqrt{2})\left(\left|\tfrac{1}{2} - \tfrac{1}{2}\right\rangle - \left|-\tfrac{1}{2}\,\tfrac{1}{2}\right\rangle\right).$$

In addition, return to equilibrium occurs as almost

TABLE IX. Initial population vector $\underline{P}^{sp}$ resulting from (a) *short* and (b) *long* saturating pulses in $LaCl_3$: ^{143}Nd at 4.2 K [see Eq. (6.4)].

	Transition saturated					
$\underline{P}^{sp}$ components	$\|30\rangle - \|40\rangle$	$\|3\pm1\rangle - \|4\pm1\rangle$	$\|3\pm3\rangle - \|4\pm4\rangle$	$\|30\rangle - \|4\pm1\rangle$	$\|4\pm3\rangle - \|4\pm4\rangle$	$\|3\pm2\rangle - \|3\pm1\rangle$
			(a) Short pulse			
P_{44}^{sp}	0.12183	0.12183	0.12510	0.12183	0.12220	0.12183
P_{43}^{sp}	0.12257	0.12257	0.12257	0.12257	0.12220	0.12257
P_{42}^{sp}	0.12325	0.12325	0.12232	0.12325	0.12325	0.12325
P_{41}^{sp}	0.12379	0.12545	0.12379	0.12410	0.12379	0.12379
P_{40}^{sp}	0.06272	0.06236	0.06236	0.06205	0.06236	0.06236
P_{30}^{sp}	0.06272	0.06308	0.06308	0.06308	0.06308	0.06308
P_{31}^{sp}	0.12711	0.12545	0.12711	0.12711	0.12710	0.12738
P_{32}^{sp}	0.12766	0.12572	0.12766	0.12766	0.12766	0.12738
P_{33}^{sp}	0.12836	0.12836	0.12510	0.12836	0.12836	0.12836
			(b) Long pulse			
P_{44}^{lp}	0.12183	0.12139	0.12680	0.12201	0.12239	0.12161
P_{43}^{lp}	0.12257	0.12212	0.12203	0.12274	0.12239	0.12235
P_{42}^{lp}	0.12325	0.12280	0.12268	0.12342	0.12308	0.12335
P_{41}^{lp}	0.12379	0.12589	0.12322	0.12422	0.12362	0.12404
P_{40}^{lp}	0.06272	0.06304	0.06208	0.06192	0.06228	0.06249
P_{30}^{lp}	0.06272	0.06377	0.06279	0.06217	0.06299	0.06321
P_{31}^{lp}	0.12711	0.12589	0.12653	0.12721	0.12694	0.12740
P_{32}^{lp}	0.12766	0.12720	0.12707	0.12784	0.12749	0.12740
P_{33}^{lp}	0.12836	0.12789	0.12680	0.12854	0.12883	0.12814

TABLE X. Relaxation rates and coefficients in the expansion of the population difference between the saturated levels as a sum of exponential decays for the (a) *short*- and (b) *long*-pulse initial states (Table IX) [see Eq. (6.10)].

	Transition saturated					
Relaxation rate $\lambda_i(sec^{-1})$	$\|30\rangle - \|40\rangle$ $C_i'(30,40)\times10^4$	$\|3\pm1\rangle - \|4\pm1\rangle$ $C_i'(31,41)\times10^4$	$\|3\pm3\rangle - \|4\pm4\rangle$ $C_i'(33,44)\times10^4$	$\|30\rangle - \|4\pm1\rangle$ $C_i'(30,41)\times10^4$	$\|4\pm3\rangle - \|4\pm4\rangle$ $C_i'(43,44)\times10^4$	$\|3\pm2\rangle - \|3\pm1\rangle$ $C_i'(32,31)\times10^4$
			(a) Short pulse			
0	7.159	16.595	32.634	11.835	3.685	2.762
28	0.000	−0.004	−0.005	−0.003	−0.617	−0.062
115	0.000	−0.123	−0.045	−0.061	−1.206	−0.687
341	0.000	−1.366	−0.022	−1.268	−0.244	−0.285
627	0.000	0.000	−9.512	−1.743	−1.026	−0.671
643	0.000	−0.003	−22.606	−0.928	−0.247	−0.158
707	0.000	−0.182	−0.442	−0.919	−0.346	−0.367
893	0.000	−14.916	0.000	−3.030	0.000	−0.530
1068	−7.159	0.000	0.000	−3.884	0.000	0.000
			(b) Long pulse			
0	7.159	16.595	32.643	11.835	3.685	2.762
28	0.000	−0.108	−0.102	−0.068	−2.255	−0.560
115	0.000	−0.798	−0.250	−0.369	−1.093	−1.423
341	0.000	−3.000	−0.041	−2.608	−0.076	−0.199
627	0.000	0.000	−9.600	−1.948	−0.170	−0.256
643	0.000	−0.004	−22.243	−1.012	−0.040	−0.058
707	0.000	−0.192	−0.395	−0.910	−0.051	−0.124
893	0.000	−12.491	0.000	−2.375	0.000	−0.141
1068	−7.159	0.000	0.000	−2.547	0.000	0.000

a pure single-exponential decay. We note also that when other transitions are saturated, relaxation rate for the $|4\,0\rangle$ and $|3\,0\rangle$ transition figures little in their return to equilibrium. These results, depending on the unique character of the $|4\,0\rangle$ and $|3\,0\rangle$ wave functions, should be true regardless of the phenomenological "dynamic crystal field parameters" used.

We see also that saturating the $|4\pm1\rangle - |3\pm1\rangle$ or $|4\pm4\rangle - |3\pm3\rangle$ transition by a short pulse re-

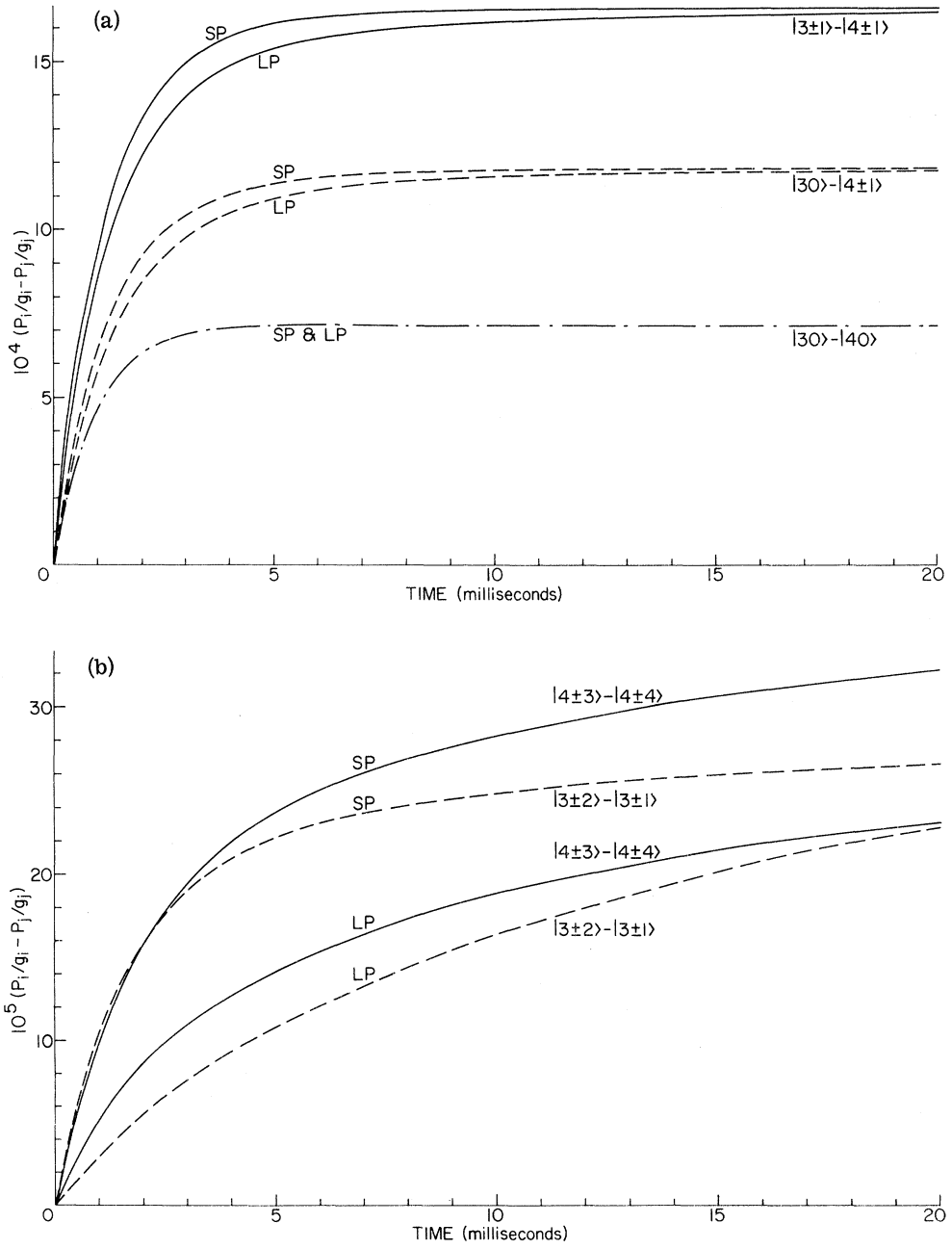

FIG. 3. Return of the population difference of two hyperfine levels $|i\rangle$ and $|j\rangle$ to its equilibrium value after both short (sp) and long (lp) saturating pulses in $LaCl_3$: Nd. (a) $\Delta F = 1$ transitions: solid line, $|3\pm1\rangle - |4\pm1\rangle$; dashed line, $|3\,0\rangle - |4\pm1\rangle$; dot-dashed line, $|3\,0\rangle - |4\,0\rangle$. (b) $\Delta F = 0$ transition: solid line, $|4\pm3\rangle - |4\pm4\rangle$; dashed line, $|3\pm2\rangle - |3\pm1\rangle$. Note change in vertical scale. Recovery from the long pulse, in which the population of all the levels has been affected, is slower than from the corresponding short pulse. This difference is particularly significant in the $\Delta F = 0$ transitions.

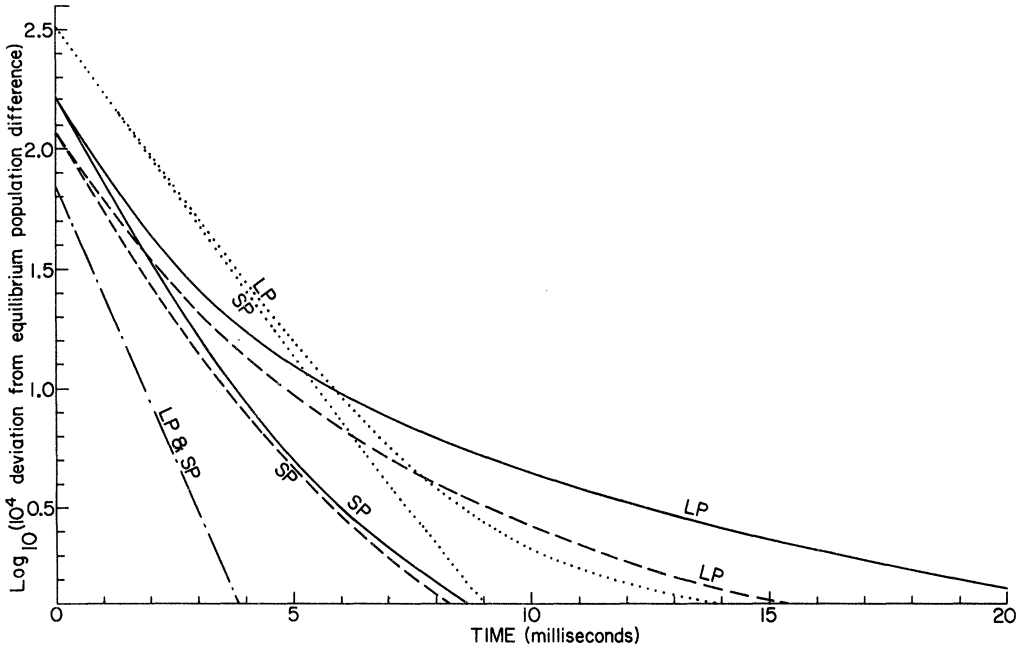

FIG. 4. Semilog plot of the deviation from the equilibrium population difference [Eq. (6.11)] for some $\Delta F = 1$ transitions in $LaCl_3$: ^{143}Nd. Such a plot specifically emphasizes the multiexponential nature of the relaxation as a purely exponential return to equilibrium appears as a straight line. The results of both short-pulse (sp) and long-pulse (lp) experiments are shown by: dotted line, $|3 \pm 3\rangle - |4 \pm 4\rangle$; solid line, $|3 \pm 1\rangle - |4 \pm 1\rangle$; dashed line, $|3\ 0\rangle - |4 \pm 1\rangle$; dot-dashed lines, $|3\ 0\rangle - |4\ 0\rangle$.

sults in a nearly single-exponential return to equilibrium (see Figs. 4 and 5 and Table IX). A long saturating pulse, however, disturbs populations in other levels, resulting in a slower, multiexponential return to equilibrium. Note also that a long saturating pulse increases the population of the

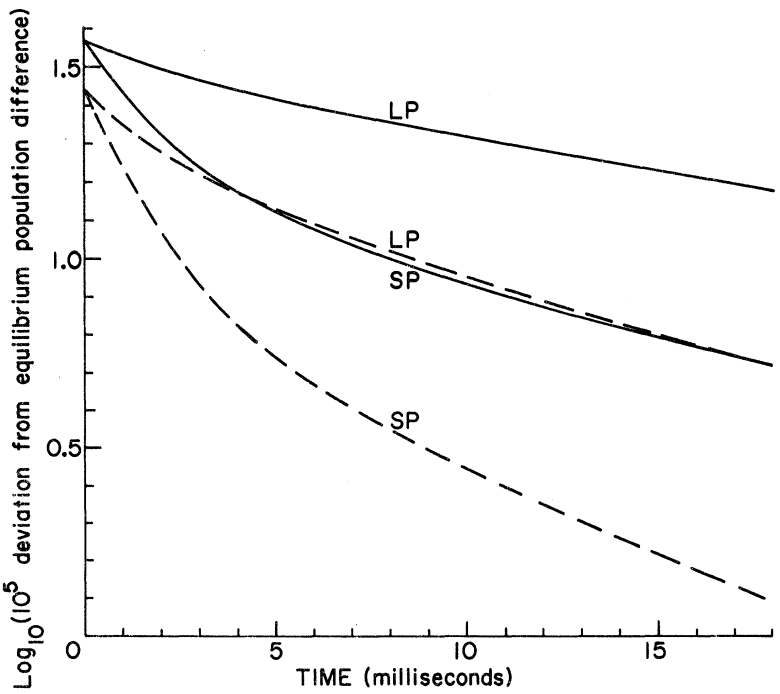

FIG. 5. Semilog plot of the deviation from the equilibrium population difference [Eq. (6.11)] for two $\Delta F = 0$ transitions in $LaCl_3$: ^{143}Nd. Such a plot specifically emphasizes the multiexponential nature of the relaxation rates: solid line, $|4 \pm 3\rangle - |4 \pm 4\rangle$; dashed line, $|3 \pm 2\rangle - |3 \pm 3\rangle$.

levels saturated at the expense of other levels.

Saturating the $|4\pm1\rangle - |3\,0\rangle$ transition results in a return to equilibrium in which at least five different relaxation pathways are significant. After saturation of the $|4\pm4\rangle - |3\pm3\rangle$ or $|3\pm1\rangle - |3\pm2\rangle$ transitions, as is typical of $\Delta F = 0$ transitions, a complex return to equilibrium also occurs. In contrast to the $\Delta F = 1$ transitions both slow and fast relaxation rates are significant.

In summary, we have presented an overview of spin-lattice relaxation for some rare-earth hyperfine levels at zero external magnetic field, based on the conventional theory of spin-lattice relaxation in rare-earth-doped diamagnetic crystals. Relaxation in such a many-level system is conveniently treated by matrix methods previously described (Sec. III). We found, for a Kramers electronic doublet coupled to half-odd-integral nuclear states via hyperfine and quadrupole interactions, an insignificant direct process increasing linearly with T, a Raman process increasing as T^7, and an Orbach process with characteristic $e^{-\Delta/kT}$ behavior. The passage to equilibrium from an arbitrary initial state can be written as a sum of $L-1$ exponentials, where L is the number of energy levels. For specially prepared initial states, return to equilibrium may be well characterized by either a single or a few exponentials depending on the method of preparation and the levels involved.

We are currently engaged in a more sophisticated theoretical approach to improve both the statistical mechanics (master equation for time evolution of the system density matrix) and the ion-lattice interaction Hamiltonian. Experiments are in progress to determine the accuracy and functional validity of the predictions described herein.

---

*Work supported by the National Science Foundation under Grant No. G. P. 29118 and by USARO-D under Contract No. DAH-CO4-7-COO27.

†National Science Foundation predoctoral fellow 1969–1972.

[1]L. E. Erickson, Phys. Rev. 143, 295 (1966).

[2]E. R. Bernstein and G. M. Dobbs (unpublished).

[3]A. Abragam and B. Bleaney, *Electron Paramagnetic Resonance of Transition Ions* (Oxford U. P., London, 1970).

[4]C. D. Jeffries, *Dynamic Nuclear Orientation* (Interscience, New York, 1963).

[5]E. R. Bernstein and C. A. Hutchison, Jr. (unpublished).

[6]*Spin-Lattice Relaxation in Ionic Solids*, edited by A. A. Manenkov and R. Orbach (Harper and Row, New York, 1966).

[7]R. Orbach, Proc. Roy. Soc. (London) A264, 485 (1961).

[8]H. A. Buckmaster, Can. J. Phys. 40, 1670 (1962).

[9]P. L. Scott and C. D. Jeffries, Phys. Rev. 127, 32 (1962).

[10]U. Fano and G. Racah, *Irreducible Tensorial Sets* (Academic, New York, 1959); B. R. Judd, *Operator Techniques for Atomic Spectroscopy* (McGraw-Hill, New York, 1963).

[11]For the direct process only we have $|\langle 4\,1|V|3\,1\rangle|^2$ and $|\langle 4\,1|V|3-1\rangle|^2$ both nonzero. To obtain the transition rate between $|4\pm1\rangle$ and $|3\pm1\rangle$, $W_{4\,1\to3\,1}$ and $W_{4\,1\to3-1}$ must be added.

[12]K. W. H. Stevens, Rept. Progr. Phys. 30, 189 (1967).

[13]A. Messiah, *Quantum Mechanics* (Wiley, New York, 1961).

[14]R. J. Elliott and K. W. H. Stevens, Proc. Roy. Soc. (London) A219, 387 (1953).

[15]R. C. Mikkelson and H. J. Stapleton, Phys. Rev. 140, A1968 (1965).

[16]F. Varsarni and J. P. Maita, Bull. Am. Phys. Soc. 10, 609 (1965).

[17]Although in $LaCl_3$: Er several excited electronic states would be expected to contribute to the Orbach process, the contribution of the second excited Kramers doublet would be a factor of $e^{-38/T}$ smaller than that of the first. This is in accord with the experimental results of Ref. 15.

[18]W. Heitler, *Quantum Theory of Radiation*, 3rd ed. (Oxford U. P., London, 1954), p. 181ff.